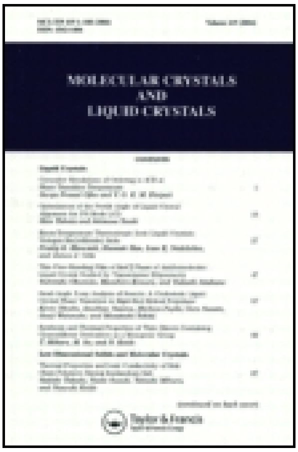

Molecular Crystals and Liquid Crystals
Publication details, including instructions for authors and subscription information:
http://www.tandfonline.com/loi/gmcl20

Disappearance of the Nematic Phase of 2,5-Disubsituted Pyridine Derivatives by Changing the Position of the Nitrogen: A Quantum Mechanical Explanation

Mihir Roychoudhury [a] & Shailendar Kumar Thakur [a]
[a] Department of Physics, DDU Gorakhpur University, Gorakhpur

Version of record first published: 07 Oct 2011

To cite this article: Mihir Roychoudhury & Shailendar Kumar Thakur (2011): Disappearance of the Nematic Phase of 2,5-Disubsituted Pyridine Derivatives by Changing the Position of the Nitrogen: A Quantum Mechanical Explanation, Molecular Crystals and Liquid Crystals, 548:1, 192-208

To link to this article: http://dx.doi.org/10.1080/15421406.2011.591673

Mol. Cryst. Liq. Cryst., Vol. 548: pp. 192–208, 2011
Copyright © Taylor & Francis Group, LLC
ISSN: 1542-1406 print/1563-5287 online
DOI: 10.1080/15421406.2011.591673

Disappearance of the Nematic Phase of 2,5-Disubsituted Pyridine Derivatives by Changing the Position of the Nitrogen: A Quantum Mechanical Explanation

MIHIR ROYCHOUDHURY*
AND SHAILENDAR KUMAR THAKUR

Department of Physics, DDU Gorakhpur University, Gorakhpur

We try to explain the causes of the disappearance of the nematic phase by changing the position of the nitrogen in 2,5-disubsituted pyridine derivatives by quantum mechanical theory. The findings explain that the electrostatic interactions along with shape anisotropy are causes of sequential appearances/disappearances of liquid crystal phases. The antiparallel or parallel orientations also play a crucial role in the formation of liquid crystal phases. The study reveals the strong alignment of mesogens in the liquid crystal phase.

Keywords Intermolecular interaction; mesophases; multicenter multipole

1. Introduction

Liquid crystals have been thoroughly investigated by both industrialists and academics because of their tremendous applications in modern technology and their interesting fundamental properties [1,2]. These molecules also possess the quality of selforganization but are relatively simple in structure although they have their own variety, such as thermotropic, lyotropic, discotic, etc. The peculiar property that makes them distinct from other molecules is that they retain order to some extent, even in a liquid state, hence the name "liquid crystals" [3]. The study of liquid crystalline properties of materials involves the study of the ability of molecules to have motional and orientational behavior at molecular level and the property of self-organization [4]. The phase morphology exhibited by these molecules has always been of interest and various theories have been proposed to understand their behavior [5,6].

The behavior of liquid crystals at molecular level has long been studied and it is now well established that the mesogeniety arises because of the asymmetry of pair potential [7–10]. Computation to understand the behavior of liquid crystalline molecules has been carried out by several researchers with different theoretical approaches [2,3,5,6,10]. Now, it is believed that the atomistic modeling of the formation of molecular complexes provides the better insight to the formation of mesogens and thereby the physics of mesophases [11–13]. G. Tiberio et al., in his atomistic modeling, attempted to predict the nematic to

---

*Address correspondence to Department of Physics, DDU Gorakhpur University Gorakhpur. E-mail: mrcgkpu@rediffmail.com isotropic realistic phase transition within the thermal agitation range [14]. His effort is very resource-demanding. It is desirable that the theory and the prediction method should be simple and not resource-demanding.

The best way to deal with mesogens at the molecular level is to take up actual molecular geometry and on the basis of electronic properties calculated using quantum mechanical methods; the intermolecular interaction energy could be calculated in a stepwise manner. However, since there is no direct method of solving the Schrödinger equation for a polyatomic system, some approximation has to be made. Furthermore, there is no single theory to evaluate properties of molecular complexes in terms of indusial molecular properties of the interacting molecules, Rayleigh–Schrödinger perturbation theory for long-range interaction appears to be suitable at least for the electrostatic and the polarization parts. For the short-range interaction parts, e.g., dispersion and repulsion, it is convenient to employ semiempirical methods. As the aim of the calculation is to take into consideration the actual geometry, the electronic properties expressed with respect to the atomic position are desirable. Thus, multicentered-multipole expansion method taking various atoms as a center seems to be a necessity not only to reduce the computational complexities but also to include the geometrical features [15]. There are many methods available for the population analysis in molecules. After considering merits and demerits of all such methods, it was finally concluded that the density functional B3LYP method using 6–31** basis set is the most suitable one for moderate size organic molecules [16]. Needless to say that although, DFT method is not strictly rigorous ab initio technique, it is compatible with experiments because of the parameters taken from experimental results.

The strategy of computation to interaction energy of various configurations for a molecular pair depends on the molecular structure under investigation. The majority of thermotropics either exhibit nematic or smectic character. These molecules are in general lath-shape, i.e., with a moderate length and linear structure. The length and breadth ratio is relatively high. The maximum overlap occurs when the planar surfaces come in contact and the molecules are aligned in same direction. This is termed as stacking. Once stacking is achieved, the two sides in the plane are still open and interaction is still possible from these sides. Such a configuration is called the inplane or planar interaction. If polar groups are projected outward, the contribution of the planar interaction may be significant. In sematogens, layer formation through inplane interactions may also be possible; hence, it is necessary to evaluate the energies of such configurations. The end of the molecules has a very small area for overlapping but if they contain the strong polar groups such as hydroxyl, C-N, etc. strong interaction between the molecules is possible, resulting into dimer formation. Such strong terminal forces increase the effective lengths of molecules and have an effect on the mesogenic character. It is, therefore, advisable to divide the interactions into three classes namely, (1) stacking, (2) inplane, and (3) terminal. It is computationally efficient and at the same time gives better insight into mesogenic character. That the interaction energy (or association energy) evaluated under the above category is a good measure of anisotropy of crystal binding forces.

When the molecular interaction occurs in such a way that several interacting segments of one molecule are weakly interacting with another molecule with great molecular overlap, it causes the energy to lower. As the temperature rises, the sequential braking of interaction occurs and gradual phase sequence appears. While two or three segments in a molecule interacting strongly with other segments does not lower the energy much. In this case, the various parts of the molecule do not come in close contact and they nearly freely vibrate from the thermal energy. In this case, they acquire the sufficient energy, and as the breaking of interaction occurs, the molecule may randomize greatly [17].

The effect on physicochemical properties of liquid crystals because of the introduction of the pyridine 2,5-disubsituted fragment into the molecular core, had attracted attention of scientists working in the field of liquid crystals. Petrov and Pavluchenko [18] have presented a comparative study of 60 compounds of this class and pointed out some peculiar structure-property relationships. It has been observed that in the case of two ring alkyl alkoxyl pyridines, the variation of length in alkyl chain or positions of hetero atoms in the ring affect the mesogenic characters significantly. The molecular structure of the 2,5-disubstituted pyridine derivatives as well as position of the nitrogen in the pyridine ring play an important role on their mesomorphic properties. The geometrical and electronic structures of the pyridine ring also play a crucial role in the intra and intermolecular interactions, which affect the packing of the molecules and influence mesophase stability.

2. Methods of Calculation

2.1 Geometry Optimization

The following procedure has been adopted uniformly for all the pyridine-derived molecules.

The molecular geometry was generated using *Gauss view*. Geometry optimization, frequency analysis and calculation of electrostatic properties were carried out using the hybrid density functional theory B3LYP with 6-31G** basis set using Gaussian03 [19]. All the structure was fully optimized without geometrical constraints

2.2 Intermolecular Interaction Calculations

The Hamiltonian of the pair of the molecule is written as

$$H' = \mathrm{H} - [H^{(a)} + H^{(b)}]$$

Where, $\mathrm{H}^{(a)}$ and $\mathrm{H}^{(b)}$ are the Hamiltonians of the free molecules a and b, where as H' is the interaction term of the molecular pair. H is the total Hamiltonian of the molecular complex containing the n electrons of the molecule a and the $n + m$ electrons of molecule b.

Where, H' is the perturbation operator; the molecular wave function is written in form of the Slater determinant formed by the constituent's atomic orbitals. The ground state molecular wave function of the molecule a is written as

$$\Psi_0^{(a)} = \frac{1}{\sqrt{n}} \det \left| \psi_1^{(a)}(1)\psi_2^{(a)}(2)............\psi_n^{(a)}(n) \right|$$

Where, $\psi_1^{(a)}(n)$ is the spin orbitals of atom n in molecule a. The molecular orbital for the molecule b similarly defined as

$$\Psi_0^{(b)} = \frac{1}{\sqrt{m}} \det \left| \psi_1^{(b)}(n+1)\psi_2^{(b)}(n+2)............\psi_n^{(a)}(n+m) \right|$$

Where, H' is treated as the perturbation operator. Applying the Rayleigh–Schrödinger perturbation method to the ground state eigenfunction of $H^{(a)} + H^{(b)}$ as the product of $\Psi_0^{(a)}\Psi_o^{(b)}$. The energy of the perturbed state obtained by standard quantum mechanical theory has electrostatic, polarization and dispersion terms. Further, to apply the perturbation on an arbitrary shaped molecule, one can define the locate charge density operator associated with two molecules. These operators are the functions of the electronic coordinates with the nuclear coordinates kept fixed. Thus, the matrix element $\left\langle \Psi_0^{(a)}\Psi_0^{(b)}|H'|\Psi_0^{(a)}\Psi_0^{(b)}\right\rangle$ is simply written as the electrostatic interactions between the two charge densities. The electrostatic interactions between these distributions will be obtained with sufficient accuracy by replacing the continuous part of charge distribution by appropriate multipole expansions at every atomic center (and the bond), which allows the considerable conceptual and computational simplification [15]. The mean charge distribution function of the molecule is defined as, $(f_{00} = \sum_\mu Z(\vec{r} - \vec{r}_\mu) - \sum_\delta \sum_\gamma p_{\delta\gamma}\chi_\delta^*(\vec{r})\chi_\gamma(\vec{r}))$, the sum of the nuclear point charge and the electronic distributions (Here, χ_δ and χ_γ are the atomic orbitals) [16]. The necessary formulae for the intermolecular interaction are given in section "2.2.1".

2.2.1 Electrostatic Interaction Energy. The $E_{el} = E_{qq} + E_{qm} + E_{mm}$ E_{qq} is the monopole–monopole interactions, E_{qm} is the monopole–dipole interactions and the E_{mm} ia dipole–dipole interactions.

$$E_{qq} = C\sum_{i,j}\frac{q_i q_j}{r_{ij}}$$

$$E_{qm} = C\sum_{i,j} q_i\vec{\mu}_j \bullet \frac{\vec{r}}{r^3}$$

$$E_{mm} = \frac{C}{r^3}\sum_{i,j}\vec{\mu}_i \bullet \vec{\mu}_j - 3(\vec{\mu}_i \bullet \hat{r})(\mu_j \bullet \hat{r})$$

Where, C is the constant and its value is 331.934 kcl/mol. The q is the net charge, and μ is the dipole moment on the atomic center on the different molecules.

2.2.2 Polarization Energy. The polarization energy, sometimes called the induction energy, of a molecule (say a), is obtained as the sum of the induced polarizations for the various bonds involved:

$$E_{ind}^{(a)} = C(-\tfrac{1}{2})\sum_u \vec{\varepsilon}_u^{[a]}\bar{A}_u^{(a)}\vec{\varepsilon}_u^{[a]}$$

Where, $\overline{\overline{A_u}}$ is the polarizability tensor of the bond u and $\vec{\varepsilon}_u^{[a]}$ is the electric field created at this bond by the surrounding molecules other than molecule (a). If the molecular charge distribution is represented by the atomic net charges q_λ^b (q is net atomic charge on atom λ in molecule b), it is found that

$$\vec{\varepsilon}_u^{[a]} = \sum_{t\neq s}\sum_\lambda {}^{(b)}q_\lambda^{(b)} \bullet \frac{\vec{R}_{\lambda u}}{R_{\lambda u}^3}$$

Where, $\vec{R}_{\lambda u}$ is the vector joining the atom λ in molecule (b) to the "center of polarizable charge" on the bond u of the molecule a.

2.2.3 Dispersive and Short-Range Repulsion Energies. The dispersion and the short-range repulsion terms are given by the semi empirical formulae of the Linord–Jhons or Buckingham type. The dispersion energy is always represented by $-A/R^6$ term, in agreement with the theoretical analysis. Kitaigorodskii adopted the “6-exp” potential and later on modified the parameters to suit all types of molecular systems. Accordingly,

$$E_{\text{disp}} + E_{\text{rep}} = \sum_{\lambda}{}^{(a)} \sum_{\nu}{}^{(b)} E(\lambda, \nu)$$

Where,

$$E(\lambda, \nu) = K_{\lambda} K_{\nu} \left(\frac{-A}{z^6} + Be^{-\gamma z} \right)$$

and

$$z = \frac{R_{\lambda\mu}}{R^0_{\lambda\nu}}, \quad R^0_{\lambda\nu} = \sqrt{(2R^w_{\lambda})(2R^w_{\nu}}$$

Where, R^w_{λ} and R^w_{ν} are the van der Waals radii of atoms λandν respectively. The parameters A, B, and γ are not dependent on the atomic species: this necessary dependence is brought about by $R^w_{\lambda\nu}$ and by the factors K_{λ},K_{ν}, that allow the energy minima to have different values according to the atomic species involved. The total energy of interaction includes the electrostatic, polarization, repulsion, and dispersion energies [15].

These calculations generated a large amount of data that are summarized in supporting information (SI) for space economy.

3. Result and Discussion

3.1 Geometry Optimization

The optimized geometries are given below with numbering scheme.

Abbreviation: Cr – crystal phase, Sm – smetic phase N – nematic phase, I – isotropic phase.

The geometry of the two molecules is different. The dihedral angles provided in Table 1 show that the two rings are making different angles and so the PD-2 becomes more nonplanar than the PD-1. The Alkoxy chain in two molecules is also taking different configurations. In PD-2, it is taking transconformation.

3.2 Inter Molecular Interaction Calculation

In the Introduction, we discussed that to investigate the various configuration space, we performed the stacking, inplane, and terminal interactions. These configurations sufficiently describe the various possibilities of interactions in the bulk speciman. These findings can provide an insight to explain the causes of phase formations in the two molecule species PD-1 and PD-2.

3.2.1 Interaction Energy. Where, (E_{qq},E_{qmi},E_{mimi}, E_{ele},E_{pol},E_{disp},E_{rep}, and E_{tot} are monopole–monopole, monopole–dipole, dipole–dipole, electrostatic, polarization, dispersion, repulsion, and total energies of interactions, respectively.)

Various energy components of interactions of pair of molecule PD-1 are tabulated in Table 2. The repulsion energy component is calculated from the exp-6 type formula and is positive compensating to total energy. The dispersion and polarization energies

Table 1. The compounds with optimized geometry, phase sequences, and important dihedral angles

Compound name	Compound structure with numbering scheme	Important dihedral angles (°)		Phase sequences (°C)
PD-1	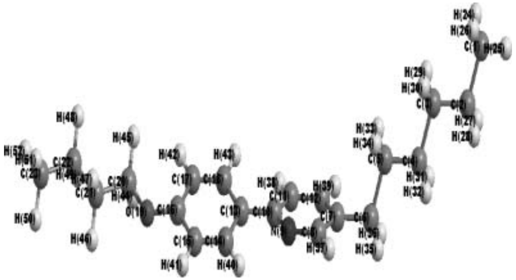	N(9)-C(10)-C(13)-C(14)	−15.96	Smectic for a small range and then nematic
		C(16)-O(19)-C(20)-C(21)	179.08	Cr-50-Sm-54-N-61-I
		O(19)-C(20)-C(21)-C(22)	179.42	
		C(20)-C(21)-C(22)-C(23)	179.63	
PD-2	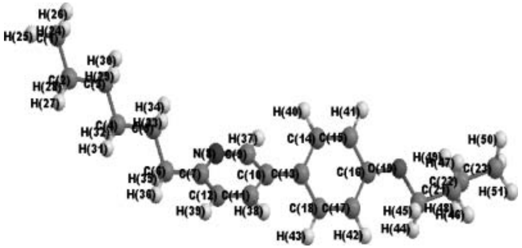	C(9)-C(10)-C(13)-C(14)	36.75°	Pure smectic
		C(16)-O(19)-C(20)-C(21)	179.97°	Cr-48-Sm-85-I
		O(19)-C(20)-C(21)-C(22)	−64.31°	
		C(20)-C(21)-C(22)-C(23)	179.269°	

Table 2. Energy (Kcl Mol^{-1}) components for various interaction configurations of molecule PD-1

	E_{qq}	E_{qmi}	E_{mimi}	E_{ele}	E_{pol}	E_{disp}	E_{rep}	E_{tot}
Configuration 1 stacking	−18.643	9.251	−1.329	−10.721	−6.591	−21.312	12.512	−26.111
Configuration 2 stacking	−25.300	12.770	−1.815	−14.346	−5.418	−17.163	9.334	−27.593
Configuration 3 stacking	−8.6296	4.758	−0.851	−4.723	−5.770	−18.678	7.862	−21.310
Configuration 4 inplane side	−0.7832	−2.415	0.337	−2.861	−2.126	−7.820	3.071	−9.736
Configuration 5 inplane side	−0.4823	−0.765	−0.239	−1.486	−3.155	−11.7	6.271	−10.070
Configuration 6 terminal side	−0.277	−0.247	−0.033	−0.5538	−0.206	−0.788	0.1727	−1.3745
Configuration 7 terminal side	−0.5121	−0.8434	−0.5803	−1.9358	−0.1615	−1.9358	0.9689	−2.2336

play the major role of providing the stability of interactions. The electrostatic components consist of three parts: monopole–monopole, monopole—dipole, and dipole–dipole. The dipole–dipole interaction is directional and plays a great role to align the molecule. In interaction for stacking, it is negative while the monopole–dipole interaction is positive and unfavorable. This monopole–dipole interaction plays a compensating role for monopole–monopole and dipole–dipole interactions. The monopole–monopole interactions are angular independent term so they are less effective in molecular alignment by their own. This depends on the charge distribution in molecule. In other words, the shape anisotropy comes to play by the monopole–monopole interactions. Not all the geometrical anisotropy comes to play role of mesophese formation until this term along with others are favorable.

Table 3 consists of various energies component of pair of interactions of molecule PD-2. As in previous interactions here, repulsion, dispersion, and polarization play similar roles. However, when we look at the electrostatic part of interaction the scenario is entirely changed here. Dipole–dipole, part of interactions, that is directional, is not favorable also; the monopole-monopole interactions are too unfavorable. Only monopole–dipole interactions are favorable. As a result the total electrostatic interactions are weakly favorable. Although, the monopole–dipole interactions are directional even then they cannot align the molecule strongly.

The electrostatic are long-range interactions and monopole–monopole, monopole—dipole, and dipole–dipole interactions are effective at various ranges. As the temperature increases in both cases, in PD-1 the sequential interaction disappears because of the monopole–monopole and the dipole–dipole interactions are favorable. The dipole–dipole interaction breaking disrupts the strong alignment, which is responsible cause for the smectic phase formation. Further, alignment is caused by the monopole–monopole attractive term that is possible cause of nematic phase formation.

In case of the PD-2, the alignment is caused by the dipole–monopole interactions. It is not strong enough. The molecule is completely smectic. As the thermal energy increases and disrupts the monopole–dipole interactions there is not any sufficient favorable energy that causes the molecular alignment to form the nematic phase. Rather the monopole–monopole repulsive term completely randomizes the molecular orientations, which causes the direct passing of the molecule from smectic phase to isotropic.

To investigate further we placed the two molecules in similer conditions of interaction and independent condition of interactions.

3.2.2 Similar Interaction Conditions. The one molecule of PD-1 is placed at origin and the other molecule of PD-1 is placed at stacking, inplane and terminal positions. The same procedure is adoped to the other molecule species, i.e., PD-2. The configuration 3 of the PD-1 molecule [Fig. 1(a)] and the configuration 1 of the PD-2 [Fig. 1(b)] are subjected under the similer condition of interaction.

The geometry of the PD-2 is a bit twisted (Table 1); the molecule does not come under close contact to each other. The hydrogen of one molecule of PD-2 is closely interacting with the nitrogen of pyridine ring as well as the hydrogen of the benzenes ring is also interacting with the pyridine ring. The oxygen one molecule of alkoxy chain is close to benzene and hydrogen of the alkoxy of one molecule close to oxygen of the other molecule in PD-2 molecular interactions.

In case of PD-1 the geometry is planer in comparison to the PD-2 molecule. Pyridine of one molecule is closely overlapping to the benzene of other molecule [Fig. 1(a)].

Table 3. Energy (Kcl Mol^{-1}) components for various interaction configurations PD-2

	E_{qq}	E_{qmi}	E_{mimi}	E_{ele}	E_{pol}	E_{disp}	E_{rep}	E_{tot}
Configuration 1 stacking	2.9636	−3.6225	0.2128	−0.4461	−2.249	−19.1707	6.7008	−15.1649
Configuration 2 stacking	1.6458	−4.2503	0.1923	−2.4121	−2.7067	−16.5022	7.281	−14.3401
Configuration 3 inplane side	1.5235	−1.5035	0.1554	0.1755	−1.8444	−9.2109	4.6592	−6.2206
Configuration 4 inplane side	1.1214	−1.2359	0.2209	0.1064	−1.4783	−8.2601	3.323	−6.3091
Configuration 5 terminal side	−1.0066	0.3467	−0.0861	−0.746	−0.4097	−2.2383	0.6867	−2.7073
Configuration 6 terminal side	−0.2075	0.1773	−0.0152	−0.0454	−0.1677	−1.4421	0.7453	−0.9099

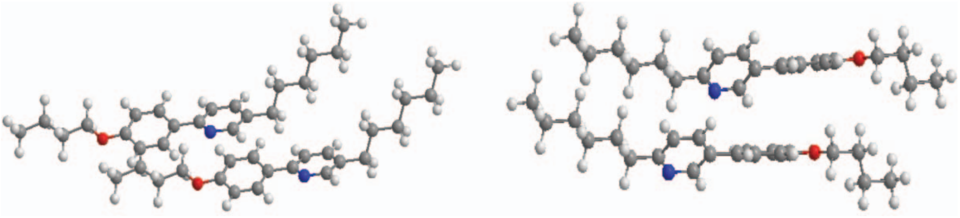

Figure 1. (a). Stacking side configuration 3 of PD-1; (b) Stacking side configuration 1 of PD-2.

3.2.3 Translational and Rotational Flexibility. In liquid crystal phase, the molecule has ability to translate and rotate about long molecular axis. The flexibility of translation and rotational explains the possible phase formations. The smecatic and nematic phase behavior at the molecular level is significantly different. The energy of thermal fluctuation is considered 4 Kcl/Mol. It is obvious from Fig. 2(a) that the molecule PD-1 translates about 1.5 Å in both sides of its mean position. The further rise of temperature may cause the translation longer in both sides to its mean position. The molecule faces rotational hindrances and rise of temperature the rotation flexibility enhanced [Fig 2(b)].

The other molecule PD-2 [Fig. 3(a)] can move along one direction. However, within the thermal fluctuation range this molecule can translate about 1.5 Å. In addition, this molecule has greater rotational range.

The parallel and antiparallel orientation plays a significant role here. The parallel and antiparallel orientation in molecule PD-2 restricts both sides of translation about the mean position of long molecular axis, whereas the parallel and anti parallel orientation in PD-1 does not restrict the translation about the long molecular axis.

3.2.4 Alignment of Molecules. The molecules in liquid crystals are aligned about a specific axis. Usually it would be about the long molecular axis. The alignment is indicated by the parameter known as the ordered parameter. Here, we do not use the order parameter to define the molecular alignment; rather, we plot a curve between energy and the rotation about the short molecular axis.

The molecule PD-1 takes the orientation in between the angle 2° in one side to the short molecular axis and about 20° to the other side of the overlapping stacking position. From Fig. 4(a), it is obvious that the repulsion energy curve is providing the similar nature to the total energy curve. That is the consequence of the geometry of the molecule. The molecule PD-1 is smectic in the range of Δ5°C temperature and nematic for a bit long

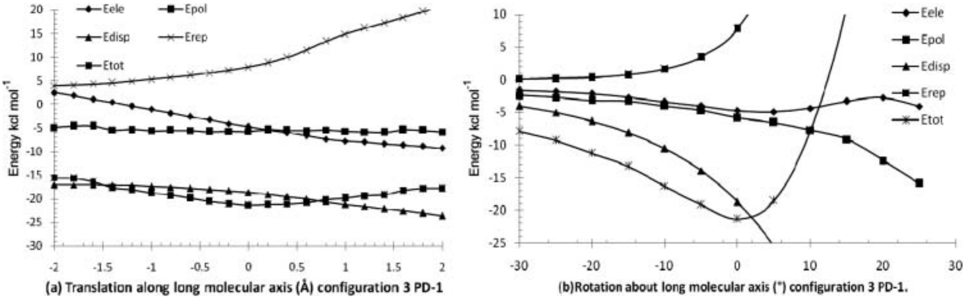

Figure 2. Translational and rotational flexibilities curves for PD-1.

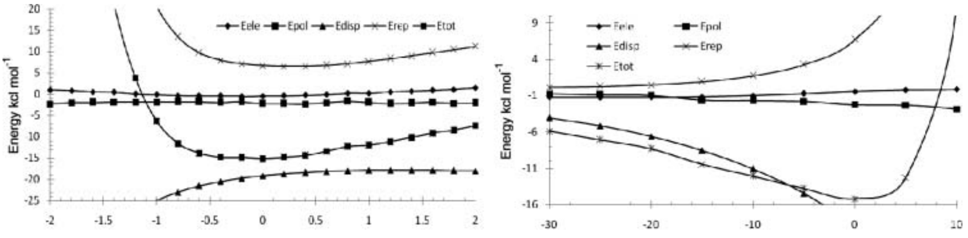

(a) Translation along long molecular axis (Å) configuration 1 PD-2. (b) Rotation about longmolecular axis (°) configuration 1 PD-2.

Figure 3. Translational and rotational flexibilities curves for PD-2.

range. The curve [Fig. 4(a)] is forming deep minimum about range of 5° from the parallel stacking orientation in this range the molecule strictly orientating parallel to each other and a smectic type of structure exist in this narrow range. The curve forms platue region from 5° to 20°, in this region, the molecule may exist in nematic phase.

The molecule PD-2 [Fig. 4(b)] takes the orientation about 2° in one side and 12° in other. This molecule is aligned very strictly parllel in stacking configuration 1 [Fig. 1(b)]. It is obvious from the above that the molecule PD-1 is a bit random with respect to the molecule PD-2. The molecule PD-2 is purely smectic in nature and that is interacting with the other molecule in such a way to form the two-dimensional (2D) structure. That 2D structure slides over each other.

To investigate further, we placed the molecule in independent condition of interactions.

3.2.5 Independent Condition of Interactions. All the configurations except the two described earlier, configuration 3 of PD-1 and the configuration 1 of the PD-2, are achieved by the independent condition of interactions.

3.2.6 Molecule PD-1 Interaction Configurations. In two of the stacking configurations [Fig. (5)], there are not any ring–ring interactions involved. In both cases, the ring is interacting with alkoxy chain. The energy of the interaction in two stacking cases is very close to each other. In the bulk specimen of the material where all the probability of interaction exist this minor difference plays a role of breaking of smectic layers. The inplane interactions are parllel and antiparllel both with oxygen in same direction and opposite direction projected outward. The configuration 5 in which oxygen is outward causes the formation of strong interaction with hydrogen of different molecule. Similar

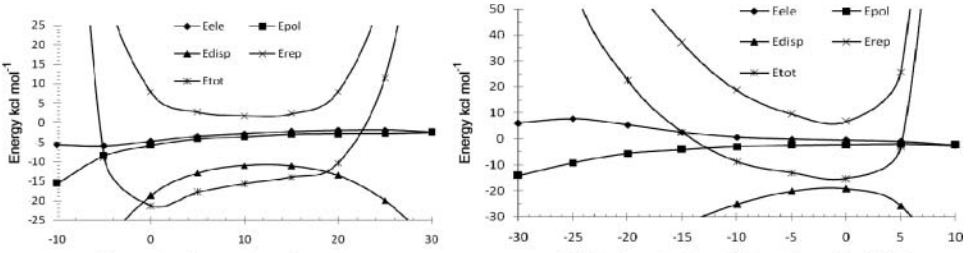

(a) Rotation about Y-axis configuration PD-1. (b) Rotation about y-axis (°) configuration1 PD-2.

Figure 4. Molecular alignment curve for PD-1 & 2.

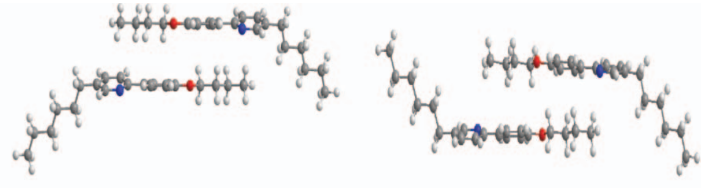

(a) Stacking configuration 1. (b) Stacking configuration 2.

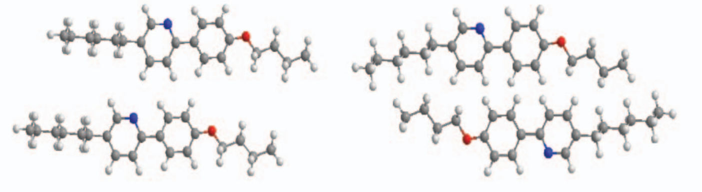

(d) Planeside configuration 4. (e) Planeside configuration 5.

Figure 5. Various interaction configurations for molecule PD-1.

types of possibilities do exist with the nitrogen of pyridine ring. The terminal interaction energy with alkoxy-alkaly chain is a bit higher than with the alkaly–alkaly chain.

3.2.6 Molecule PD-2 Interaction Configurations. In stacking configuration, the alkoxy chain interacts with the pyridine ring. Because of the twisted geometry of the molecule, the benzene ring does not come in close contact with each other. The two-plane-side interactions

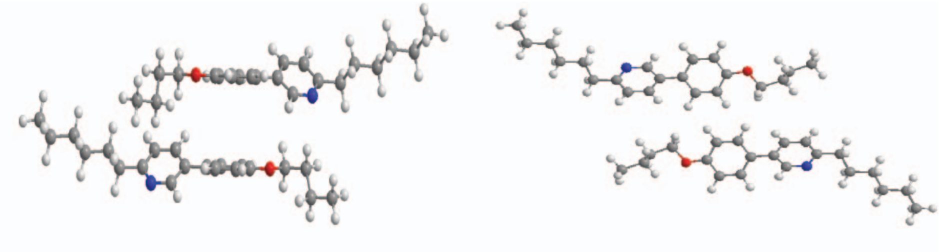

(b) Stacking side configuration 2. (c) Plane side configuration 3.

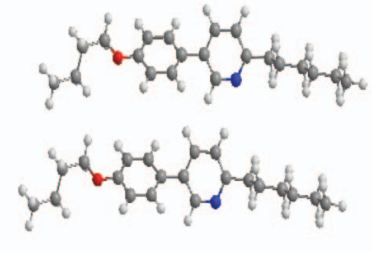

(d) Plane side configuration 4.

Figure 6. The various configurations interaction of molecule PD-2.

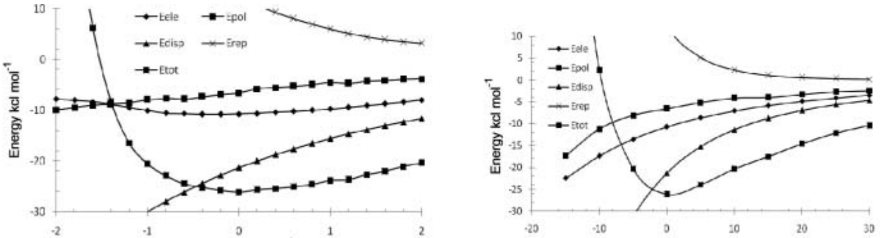

(a)Translation about long molecularaxis (Å) configuration 1.

(b) Rotation about long molecular axis (°) configuration1 .

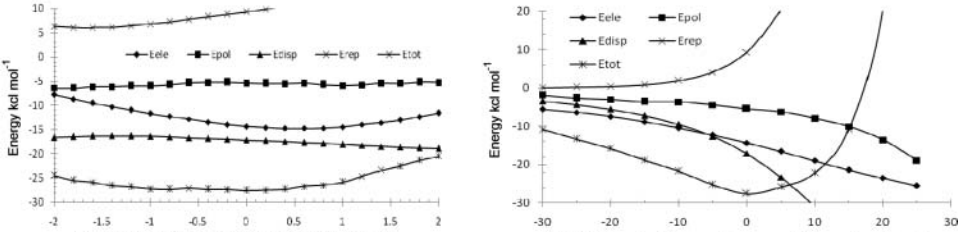

(c) Translation along long molecular axis (Å) configuration 2.

(d)Rotation about long molecular axis (Ã) configuration 2.

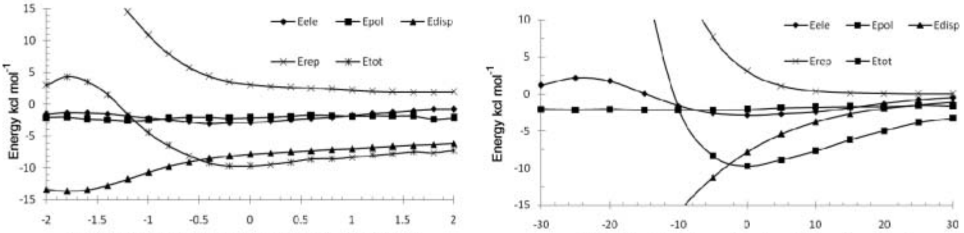

(a) Translation along long molecular axis (Å) configuration 4.

(b) Rotation about long molecular axis (°) configuration 4.

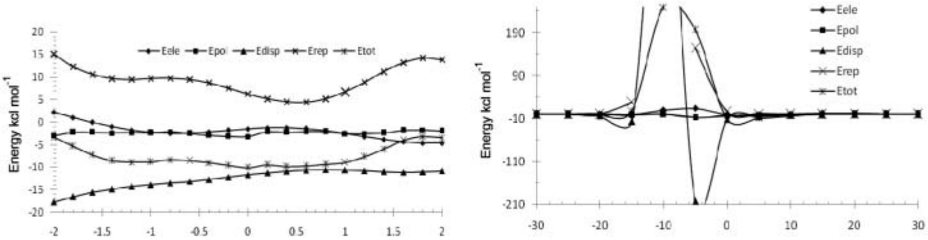

(c) Translational about long molecular axis (Å) configuration 5.

(d) Rotation about long molecular Axis (°) configuration 5.

Figure 7. Translational and rotational flexibilities curves for PD-1.

are parallel and antiparallel to each other. In the terminal interaction, the alkoxy–alkaly chain has a bit higher energy.

3.2.7 Translation and Rotational Freedom PD-1. The configurations 1 and 2 both are stacking configurations. In configuration 1, the molecule can translate about 2 Å distance nearly at expense of Δ4 Kcl Mol^{-1} energy though the configuration 2 translates more than the 2 Å distance. The configuration 2 translational curve is a bit asymmetric while the configuration 1 is completely asymmetric about its mean position. The antiparallel arrangement can make the stacking layer stable at low or very short range of temperatures. In both stacking configurations, the nature of the curve is a bit similar. The planer interaction curves of the translational freedom allow the molecule to move nearly the same

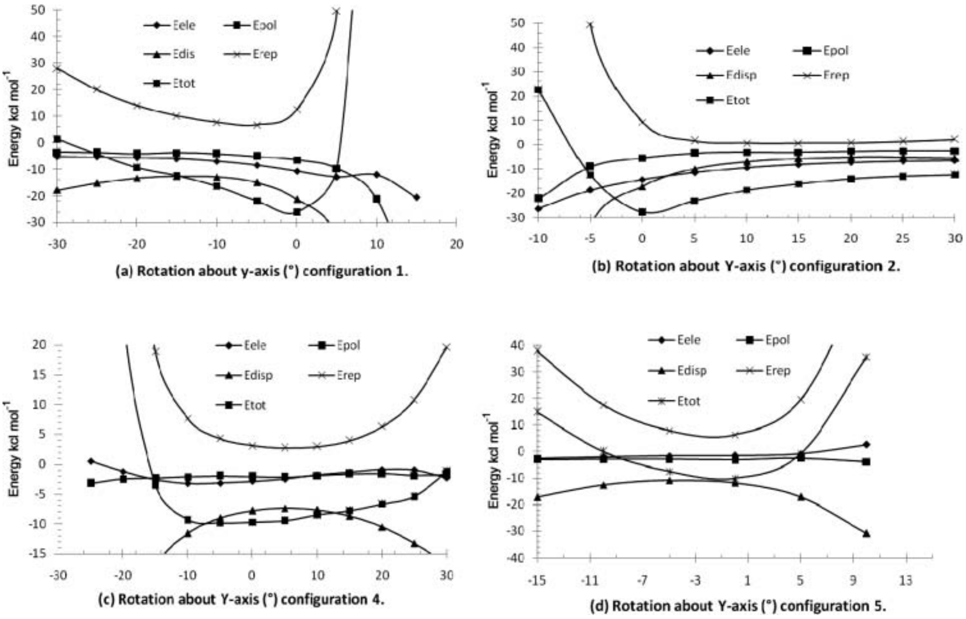

Figure 8. Molecular alignment curve for PD-1 for various configurations.

amount as that of the stacking configurations. The configuration 4 curve is asymmetric while the configuration 5 translational curve is symmetric about the mean positions. The configurations 5 the molecule faces a potential barrier for a very short range in rotation. In this region, the rotation is not usual.

3.2.7 Molecular Alinment of Molecule PD-1. In stacking configuration 1, the molecule swings about 10° to its parallel stacking configuration in one side about its mean position. Further, rise of thermal energy causes the gradual rise of randomness in orientation of the molecule, whereas in configuration 2, the molecule randomizes in one side faster than the other side. This also indicates the gradual randomness of the molecule takes place as the temperature increases. In these two stacking configurations, a sharp deep is not observed, which indicates the smectic behavior of the molecule, although a slight indication exists in configuration 1. In planeside interactions, the molecule is within the range ±15° in configuration 5 and -10° to less than 30° to its mean position of parallel orientations. So, it indicates that any interaction that causes strong parallel orientation causes the other orientations to be parallel, also, provided that the thermal energy does not distrub it.

3.2.8 Translational and Rotational Flexibility of PD-2. The configuration 2 is stacking in which the molecule translate along the one side of mean position about its long molecular axis with nearly $\Delta 4$ Kcl mol^{-1} of energy. The rotation about the long molecular axis is permissible to the large extant for the same amount of energy expense as that of in translation. In two planeside interactions (Fig. 8) the translation in one side from the mean position along long molecular axis is observed. The difference of the two plane sides (configurations 4 and 5) interaction energy is also negligibly small. So, the parallel and antiparllel orientation combination makes the smectic layer stable. The rotation in

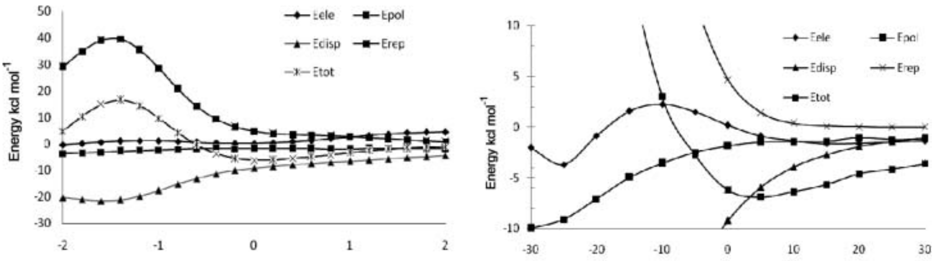

(a) Translation along X-axis (Å) configuration 3.

(b) Rotation about long molecular axis (Å) configuration 3.

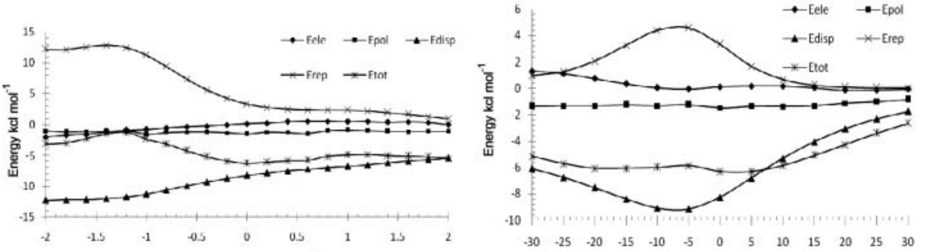

(c) Translation along long molecular Axis (Å) configuration 4.

(d) Rotation about long molecular axis (Å) configuration 4.

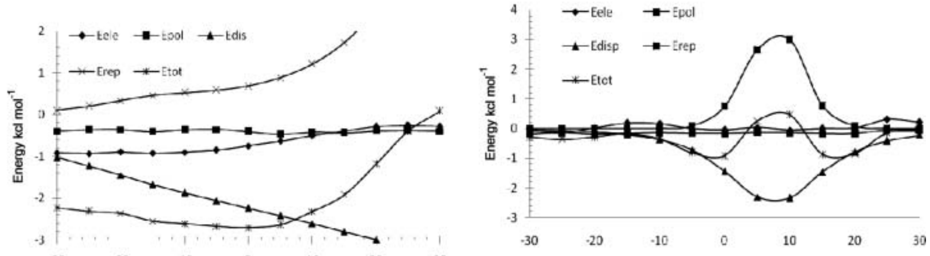

(k) Rotation about long molecular axis (°) configuration 5.

(m) Rotation about long molecular axis (°) configuration 6.

Figure 9. Translational and rotational flexibilities curves for PD-2.

configuration 4 is quite smooth in comparison to the configuration 3. In the terminal interactions, the molecule faces some hinderance but as the thermal energy increases it weakens the terminal interaction and the molecule start rotation.

3.2.9 Molecular Alignment of Molecule PD-2. Configuration 2 is stacking in which the molecule is highly aligned in very narrow range of energy (Fig. 9). The molecule randomized only in one direction from the mean position of parallel alignment. The two stacking configuration (configurations 1 and 2) are parallel and antiparallel and it is true for configurations 3 and 4, inplane interactions. The energy differences between the stacking (configurations 1 and 2) as well as inplane (configurations 3 and 4) are small. The planer interactions (configurations 3 and 4) are not very directional as a small amount of energy can make the molecule to take orientation from −30° to 5° and −20° to 30° in configurations 3 and 4, respectively. Only antiparallel and parallel combination makes the smectic phase more stable.

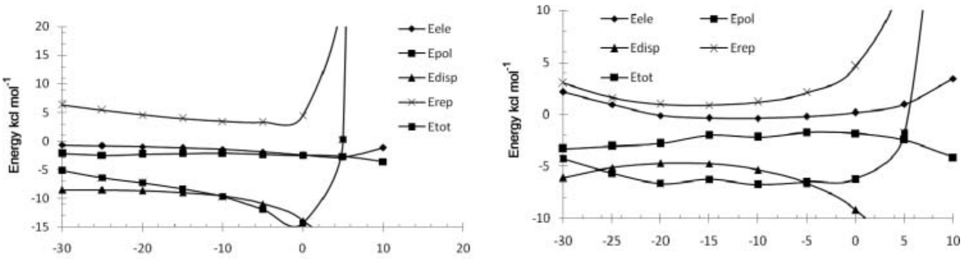

(a) Rotation about Y axis (Å) configuration 2.

(b)Rotation about long Y-axis (°) configuration 3.

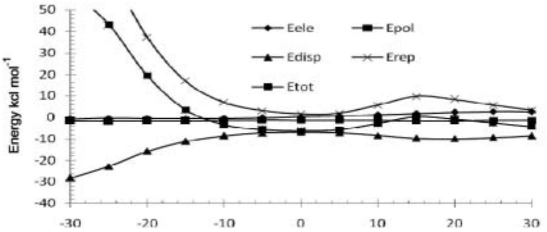

(c) Rotation about Y-axis (°) configuration 4.

Figure 10. Molecular alignment curve for PD-2 for various configurations.

4. Conclusion

The electrostatic interactions along with other factors are responsible for sequential phase appearances/disappearances in mesogens. The shape anisotropy plays its role along with electrostatic interactions to form the liquid crystal phase formation. The parallel and antiparallel alignment is crucial to determine the phase formation.

Acknowledgment

The authors are thankful to the Dept. Science & Technology for providing the computational facilities under DST-FIST grant No. SR/FST/PSI?204.

References

[1] Semenza, P. (2007). *Nat. Photonics*, *1*, 276–278.

[2] Laventovich, O., Pasmi, P., Zannoni, C., & Zumer, S. (Eds.). (2001). *Defects in liquid crystals: Computer Simulations Theory and Experiments*, Kluwer: Dordrecht.

[3] Dunmur, D. A., & Singh, S. (2002). *Liquid Crystals*, World Scientific: Singapore.

[4] Chandrasekhar, S. (1992). *Liquid Crystals*, 2nd Ed., Cambridige University Press: Cambridge.

[5] Priestley, E. B., Wojtowicz, P. J., & Sheng, P. (Eds.). (1975). *Introduction to Liquid Crystals*, Plenum Press: New York/London.

[6] de Gannes, P. G., and Prost, J. (1993). *Physics of Liquid Crystals*, 2nd Ed., Oxford University Press: Oxford.

[7] Roychoudhury, M., Ojha, D. P., & Sanyal, N. K. (1994). *Ind. J. Pure & Appl. Phys.*, *32*, 440.

[8] Ojha, D. P., Kumar, D., & Roychoudhury, M. (1995). *In Proc. Nat. Acad. Sci. India*, *65A*, 115, Allahabad, India.

[9] Roychoudhury, M., & Kumar, D. (1996). *Materials Sci. Forum Transtec Publ. Switzerland*, *13*, 222–223.

[10] Bhadur, B. (Eds.). (1990). *Liquid Crystals Applications and Uses*, Vol. 1, World Scientific: Toronto, Canada.

[11] McDonald, A. J., & Hanna, S. (2004). *Mol. Cryst. Liq. Cryst.*, *413*, 2271–2280.

[12] McDonald, A. J., & Hanna, S. (2006). *J. Chem. Phys.*, *124*, 164906.

[13] Pelaez, J., & Wilson, M. R. (2006). *Phys. Rev. Lett.*, *97*, 267801.

[14] Tiberio, G., Muccioli, L., Berardi, R., & Zannoni, C. (2009). *Chem. Phys. Chem.*, *10*, 125–136.

[15] Claverie, P. (1978). Elaboration of approximate formulas for the interactions between large molecules: Applications in organic chemistry. In: B. Pullman (Ed.), *Intermolecular Interactions, From Diatomic to Biopolymers*, John Wiley & Sons Ltd., pp. 69–305.

[16] Jensen, F. (2007). *Introduction to Computational Chemistry*, 2nd Ed., John Wiley & Sons Ltd., Chichester, pp. 217–295.

[17] Siegbahn, P. E. M. (2003). *Quaet. Rev. Biophys.*, *36*, 91.

[18] Becker, O. M., & Watanabe, M. (2001). Dynamic methods. In: O. M. Backer, A. D. MacKerell, Jr., B. Roux, & M. Watanabe (Eds.), *Computational Biochemistry and Biophysics*, p. 49.

[19] Petrove, V. F., & Pavluchenko, A. I. (2002). *Mol. Cryst. Liq. Cryst.*, *383*, 63–79.

[20] Frisch, M. J., Trucks, G. W., Schlegel, H. B., Scuseria, G. E., Robb, M. A., Cheeseman, J. R., Montgomery, J. A., Jr., Vreven, T., Kudin, K. N., Burant, J. C., Millam, J. M., Iyengar, S. S., Tomasi, J., Barone, V., Mennucci, B., Cossi, M., Scalmani, G., Rega, N., Petersson, G. A., Nakatsuji, H., Hada, M., Ehara, M., Toyota, K., Fukuda, R., Hasegawa, J., Ishida, M., Nakajima, T., Honda, Y., Kitao, O., Nakai, H., Klene, M., Li, X., Knox, J. E., Hratchian, H. P., Cross, J. B., Bakken, V., Adamo, C., Jaramillo, J., Gomperts, R., Stratmann, R. E., Yazyev, O., Austin, A. J., Cammi, R., Pomelli, C., Ochterski, J. W., Ayala, P. Y., Morokuma, K., Voth, G. A., Salvador, P., Dannenberg, J. J., Zakrzewski, V. G., Dapprich, S., Daniels, A. D., Strain, M. C., Farkas, O., Malick, D. K., Rabuck, A. D., Raghavachari, K., Foresman, J. B., Ortiz, J. V., Cui, Q., Baboul, A. G., Clifford, S., Cioslowski, J., Stefanov, B. B., Liu, G., Liashenko, A., Piskorz, P., Komaromi, I., Martin, R. L., Fox, D. J., Keith, T., Al-Laham, M. A., Peng, C. Y., Nanayakkara, A., Challacombe, M., Gill, P. M. W., Johnson, B., Chen, W., Wong, M. W., Gonzalez, C., & Pople, J. A. (2004). Gaussian 03, Rev. D.01, Gaussian, Inc., Wallingford, CT.